Seismic tests on three shaking tables of a 1:8 irregular bridge model in support of design Eurocode 8

Mario Casirati
Head, Structural Testing and Survey Dept., ISMES, Bergamo, Italy

Giorgio Franchioni
Structural Testing Laboratory, ISMES, Bergamo, Italy

Stathis N. Bousias
Dept. of Civil Engineering, University of Patras, Patras, Greece

Paper No. 2047. (quote when citing this article)
Eleventh World Conference on Earthquake Engineering
ISBN: 0 08 042822 3

ABSTRACT: The inelastic design criteria for two 1:8 scale model bridges with three piers of different height are investigated, together with the results of static tests carried out on the shorter pier alone, and the dynamic tests performed by means of the simultaneous use of three shaking tables. The seismic tests have been carried out with synchronous motion of the tables. Asynchronous motion tests will be also performed.

Keywords

Eurocode 8, geometrical irregularity, experimental tests, physical model, earthquakes, seismic simulation, bridge, pier, tests, dynamics, plasticity, ductility, behaviour factor, shaking tables.

1 INTRODUCTION

In regions of moderate to high seismicity, a bridge structure should be designed so as to provide it with reliable means to dissipate significant amounts of the seismic energy induced. The capacity design ap-proach introduced in Eurocode 8 ensures the hierarchy of strengths of the various structural components, and leads to an intended mechanism of energy absorption through plastic hinge formation and avoidance of brittle failure modes. In the case of bridge structures, the optimum post elastic seismic behaviour is achieved if plastic hinges develop approximately simultaneously in as many piers as possible, so providing the closest approximation to a theoretical elasto-plastic behaviour. If the piers are not of equal length (i.e., in steep sided valleys), the shorter and stiffer ones sustain higher forces, and therefore demand the highest local ductility, thus leading to non simultaneous yielding in the piers. In the transverse direction this phenomenon leads to substantial deviation between the results of the actual non linear response of the bridge and an "equivalent" linear dynamic analysis. As in EC8 behaviour factors are employed to reflect the actual ductile capacity of the piers in the post elastic regime, it remains to be examined if such ductility levels can be indeed supplied by piers designed according to the provisions of EC8.

Examination of the ductility demand as well as of the actually available structural ductility of bridge piers was sought through shaking table tests on irregular bridge models subjected to strong seismic motions in the direction transverse to the longitudinal deck axis. Additionally, bridge piers behaviour was investigated for the case of a synchronous base excitation. This emanates from the fact that the possibility of discontinuous ground displacements at the base of the piers (due to non-homogeneous soil formations, or due to the presence of potentially active tectonic faults) is accomodated in EC8 by providing suitable separation joints. It is, therefore, of interest to study the consequences of deviations from code provisions.

Laboratory tests were preceded by a series of numerical analyses with simplified non linear dynamic models.

This research is carried out within the frame of the Human Capital & Mobility Program of the EU.

2 CONCEPTUAL DESIGN

2.1 *Prototype structure*

A typical multi-span continuous deck motorway bridge was selected to be tested (Fig. 1a). It comprised four identical spans, 50 m each, supported at three piers and at the abutments. The piers were of hollow rectangular cross-section with structural irregularity in elevation with respect to the heights. Piers were of 7, 14 and 21 m height, with the shorter one located at midspan, being also the one to be more vulnerable to the seismic motion due to its higher stiffness. The detailing of the piers was carried out based on the EC8 provisions for Structures in Seismic Regions.
The bridge deck was 14m wide with hollow-core prestressed cross-section supported at the abutments in such a way as to allow rotation at the extremities. The deck is supported on the piers by means of special unidirectional and multidirectional supporting devices.
For comparison of testing methods, two similar bridges, one with the same configuration as the above, and one with regular configuration (piers of 14, 21, and 14 m height, respectively) were planned to be tested at the European Laboratory for Structural Assessment, at Ispra, using the Pseudo Dynamic Testing method.
The experimental study carried out at Ismes comprises the following phases:

1. Bridge model specimen definition
2. Material characterization
3. Pier - deck design
4. Uniaxial flexure test on bridge shortest pier
5. Tests of the full model on three shaking tables with synchronous and asynchronous excitations.

2.2 *Model bridge specimen*

Due to limitations of hydraulic systems in supplying the power required to excite dynamically a full scale specimen of the mass of a bridge, scaled down specimens are commonly used in shaking table laboratory tests. Model properties are defined by the necessity of proper reproduction of the stresses in the bridge elements (mainly in the piers), of the mechanical characteristics of the model material, of a significant seismic excitation, as well as of the testing equipment available for carrying out tests on a model of significant dimensions. The characteristics of the three shaking tables available are included in Table 1.

Table 1 Shaking table main characteristics

	MASTER	ARIETE	BIAX
size (m)	4×4	2,5×4	1,55×1,25
frequency range (Hz)	0-120	0-60	0-60
max. stroke (mm)	200	200	150
max hor. veloc. (mm/s)	600	500	300
max. vert. veloc. (mm/s)	450	500	300
dead weight (kN)	100	45	6
max payload (kN)	500	500	300
max horiz. force (kN)	500	150	250
max vertical force (kN)	600	150	250
max over. mom. (kNm)	300	300	200
degrees of freedom	6 (*)	3 (=)	2 (*)

(*) : simultaneous
(=) : non-simultaneous

With regard to the simulation of the abutments, ideally they should have been fixed on the shaking tables or to the laboratory floor. Neither was possible, so two cantilevers of 3 m length each were left on each side (Fig. 1b).
To reduce distortions and possible uncertainties with respect to the material mechanical characterstics, especially for specimens entering the post-elastic regime, the same materials (in terms of strength and stress-strain behaviour) as the prototype were adopted (micro concrete and commercial steel reinforcing bars).

To correctly reproduce in the model the forces developed in the prototype, whilst maintaining the loads acting on the shaking tables within their performance limits (i.e., thrust capacity of the actuators and overturning moment compensation), an appropriate scale factor must be adopted. With the adoption of a scale factor of 8, the available equipment capacities are not exceeded, and, at the same time, a substantial model can be tested free of material distortions and measurement problems.
Another modification in the model geometry was the adoption of an I section for the piers by simply joining the two opposite wider sides of the section (Fig. 1b), owing to the fact that the thickness of the pier cross section in the 1:8 model would otherwise have been 50 mm, raising questions both about specimen construction and possible out of plane distortions of the sides of the hollow cross-section.

3 MATERIAL CHARACTERIZATION

Concrete strength was determined by compression tests on seven concrete test cubes (10 cm side), and a mean value of 56,40 MPa was obtained. Additionally, steel bar specimens were subjected to uniaxial tension testing for determination of the properties of the material used in the bridge model. Pull-out tests on steel bars with one end embedded in concrete, were also performed.
Design and detailing of the piers was performed along the lines of the EC8 provisions. Simulation of the reinforcement from prototype to model was performed by scaling the steel area required in the prototype rather than scaling the bar diameters. All reinforcing details are shown in Fig. 2.
The bridge deck was designed also according to EC8 taking into account the special loading conditions it might be subjected to during subsequent phases of the installation procedure. The deck was constructed in three pieces with special end details, which were assembled and post-tensioned with a 2000 kN axial force, before being laid on the top of the piers. Special care was exercised during the assembling process to avoid loading the piers in any way.

4 UNIAXIAL FLEXURE TEST OF SQUAT PIER

Testing of the full bridge model was preceded by an experimental verification of the behaviour of the shortest pier, being the one expected to exhibit the highest ductility demands during the bridge response. The 0,90 m high pier tested, of I cross-section, was identical to the shorter of the piers used in the bridge model structure (Fig. 1b), and was monolithically cast with a heavily reinforced concrete base. Pairs of increasing amplitude, displacement controlled, cycles of 0,5 mm, 1,5 mm, 3,75 mm, 7,5 mm and 15 mm size (Fig. 3), were applied at the top of the column by means of a servocontrolled actuator. The axial load was simulated through a 150 kN concrete block located at the top of the pier by means of a swivel.
Instrumentation comprised the following: (a) two sets of extensometers on the external face of the flanges, at heights 2 cm, 10 cm, 30 cm and 50 cm from the base of the pier. At the lower two levels (2 cm and 10 cm), sets of 3 extensometers were placed, symmetrically with respect to the major axis of the section; (c) two strain gages mounted on longitudi-nal steel bars located in one of the flanges; (d) a set of displacement transducers, used to monitor the rotations and placed on both flanges, 10 cm from the base of the pier; and (e) a set of horizontally placed LVDTs at 10 cm, 30 cm, 50 cm, 77 cm and 90 cm from the base, which permitted the reproduction of the deflected shape of the specimen. As the squat pier specimen was expected to exhibit significant shear dominated diagonal cracking, a pair of displacement transducers diagonally placed between the levels of 2 cm and 45 cm from the base, allowed the determination of shear deformations and, indirectly, the flexural ones.
During testing, which was performed at a rate of about 0,02 mm/sec, cracking of the pier started at a displacement level of 0,75 mm (0,08% drift) and was of flexural type with cracks extending only within the flange width. Further increase of transverse displacements led to crack propagation with an inclination slightly less than 45°, thus signalling that shear effects were taking over the response. After the formation of the diagonal cracks full truss mechanism develops in the absence of arching action, since the latter can be activated only after complete loss of bond transfer which in this case was not observed. Diagonal cracking causes an increase in the tensile force in the flexural steel, greater than that required to resist the external moment at a section.
Due to the presence of axial compression (normalised axial load of about 0,04), high concrete strength (mean compressive strength 56,4 MPa), low ratio of web to flange width (equal to 2,1), the diagonal cracks tend to be flatter than 45°. Furthermore, as has already been shown by past studies (Muguruma, 1990, Sugano, 1990),

increased concrete compressive strength decreases the effectiveness of transverse reinforcement and shows a rapid decrease in load carrying capacity after maximum load is reached. Sufficiently high yield strength of the stirrups is needed to provide an essentially flat post-peak region (Sugano, 1990), while reinforcement grade does not affect appreciably the behaviour.
No concrete spalling during test was observed. The inclined cracks were rather spread and extended, at the maximum displacement level applied, up to the underside of the compression flange, implying that a portion of the web that may be required to carry compression could not be utilized for this purpose.
Yielding of flexural reinforcement as a result of cyclic reversed loading lead to rapid deterioration of concrete shear-resisting mechanisms. Failure was manifested by rupture of two of the longitudinal steel reinforcing bars, as indicated also by the abrupt drop in resistance at maximum displacement (15 mm, or, 1.6% drift) in the force-deflection diagramme (Fig. 3). No buckling of the longitudinal reinforcement was observed. Stiffness reduction depended primarily on the magnitude of the previously imposed loading rather than on the number of cycles applied. The hysteretic loops obtained are rather thin and pinched at the zero force level, implying a reduced hysteretic energy dissipation capacity. Deflection at yield was estimated to about 7 mm, leading to a ductility level of approximately 4. Test results are shown in figs 3.

5 TESTS ON FULL BRIDGE MODEL

5.1 *Model instrumentation*

The bridge model instrumentation comprised :
(a) thirteen accelerometers placed transversely to the deck, measuring horizontal deck acceleration;
(b) ten accelerometers placed on the deck to measure vertical acceleration;
(c) three accelerometers, one at the top of each pier, placed transversely to the bridge longitudinal axis;
(d) a series of extensometers at the base of each pier and on both faces of the piers' cross section;
(e) three sets of LVDTs, one on each pier. Each set comprised four LVDTs, all placed 30 cm apart, on the same vertical plane, transversely to the longitudinal bridge axis. The last LVDT of each series was located 10 cm below the top of each pier;
(f) A pair of LVDTs on section flanges, 10 cm below the top of each pier, along the logitudinal bridge axis;
(g) Shaking tables' forces and displacements.

5.2 *Dynamic characterization tests*

The dynamic characterization testing programme comprised four phases. In the first, a static force of 10 kN was applied alternatively at the top of each pier transversely to the longitudinal bridge axis. Snap-back tests were then performed in the second phase, on each pier, with a 10 kN force. In the third phase, sinusoidal low amplitude (0,02 g) base excitation tests were applied alternatively at each pier, in the range 1-60 Hz. Finally, transversal and vertical excitation was applied by means of an electromechanical device in the range of 1-100 Hz, at quarter-length positions along the bridge deck.
The results of the tests are summarized in Table 2, in which missing values for frequency correspond to modes not excited by the specific test, while missing damping values are due to the presence of coupled modes in the transfer function.

6. SYNCHRONOUS SEISMIC EXCITATION

The multispan bridge model was subjected to seismic excitation imposed through the shaking tables in the transverse direction with respect to the bridge longitudinal axis. Based on the spectrum defined in Eurocode 8, the reference spectrum for soil type B was chosen. A spectrum in the frequency domain was then synthesized by the control system and an artificial accelerogram of total duration of 7 sec was generated (Fig. 5). It is noted that, due to control problems, the frequency range was decreased within 0-35 Hz while strict conformity to similitude requirements would dictate a range of 0-90 Hz. Additionaly, input accelerogram duration was extended to 7 sec, as opposed to 3 sec dictated by similitude requirements.
Seismic testing was performed at levels of increasing synchronous excitation, starting from -12 dB, -6 dB, continuing with 3dB increments up to +6 dB, and performing a +10 dB and a +15 dB level tests at the end.

The test train from 0 dB to 15 dB was repeated once again, as no appreciable damage was evidenced in the first test series. As absolute synchronization (in terms of amplitude, duration, starting time and frequency content) is almost impossible, in these tests synchronization consisted of equal excitation duration, identical reference accelerogram and same starting time, and was indeed satisfactory (Fig. 6).
While at low frequency values the spectra obtained approximate satisfactorily the reference ones, large deviations between reference and actual spectra were observed at high frequencies, with the maximum deviation occurring at the BIAX shaking table. The latter, carrying the majority of the deck weight, was the most difficult to control.
Acceleration values recorded both in the horizontal and the vertical directions were higher at the deck extremities. Furthermore, owing to small tolerances in the support devices used, high acceleration peaks were recorded by the accelerometers at the top of the piers due to thrusting of the deck on the columns during seismic motion. The latter phenomenon deteriorated with increasing excitation level. Another general observation made from the acceleration signals recorded, after being transferred in the frequency domain, is that the bridge model responds primarily in frequencies lower than 10 Hz.
During testing, significant deck rotations along its longitudinal axis were observed, especially at high excitation levels. Limited cracking was evidenced on the piers as long as the deck was still supported on them. After lifting up the deck, flexural cracks of considerable width were found at the sections' flanges, mostly at the 2,7 m pier, revealing also the fracture of one of the corner reinforcing bars at this pier. Diagonal cracking was also evident. The least damaged of the other two piers, was the 0,9 m high one, on which only hair cracks were manifested. The overall damage on the piers was consistent with the conclusions drawn from the comparison of the calculated resistance of each pier (37 kN, 56 kN, and 150 kN for the 2,7 m, 1,8 m and 0,9 m high piers, respectively), and the actual maximum force applied at the top of each pier during test.
Displacement measurements at the top of the piers showed that no torsional movement developed. The deflected shapes of the columns, though, reconstructed by displacements taken at several locations along the piers' height, revealed that at the top of the 2,7 m high pier the support device exerted a restraining moment in the opposite sense than the one due to inertial forces.
Deformation measurements taken at the bottom of the piers showed that the ultimate concrete strain in compression was not exceeded during testing, thus, no spalling of the concrete cover was observed. Similar compressive deformations were recorded at the 1,8 m and 0,9 m high piers, while at the 2,7 m high pier much higher values were observed.
The state of damage of the bridge after test was assessed by performing a low-level sweep-sine test with frequencies varying between zero and 40 Hz. As expected, decreased pier stiffness due to seismic excitation led to shifting of the local maxima of the frequency response functions at lower frequencies (Fig. 7). The frequency shift (1-1,5 Hz, approximately), is not the same in the whole range, being higher at low frequencies where the response is mainly due to the behaviour of the piers. It should be noted, however, that had the characterization test been performed at amplitude high enough to cause crack opening, the frequency shift would have been much higher.

7 CONCLUSIONS

A 1:8 scale bridge model with three piers of unequal height, each one supported on a shaking table, was subjected to identical seismic excitations applied simultaneously at all three shaking tables in the transverse direction with respect to the bridge longitudinal axis. Both specimens and applied excitation were designed so as to conform with the requirements of EC8. The main purpose of the test was to investigate pier behaviour in cases of such irregular bridge configuration. Induced excitation reached at base accelerations as much as 0,56 g, while satisfactory synchronization of input signals was achieved. Bridge piers performed well sustaining without problems interstorey drifts as high as 0,6%, 0,7% and 1,3%, for the 1,8 m, 0,9 m and 2,7 m high piers, respectively. Damage was mostly located at the highest pier, owing to the fact that having left the abutments free, the largest displacements developed mainly at the external piers, the central and shorter one being almost a node during excitation. The level of bridge damage was assessed by a dynamic characterization test which showed a shift of natural frequencies by about 1-1,5 Hz towards lower values.
In the next few months, asynchronous tests on the model (after replacing the damaged piers) will be carried out. A more detailed analysis of the results, with the comparison of the different models studied will be the subject of a subsequent paper.

REFERENCES

Eurocode 8 - Part II. 1994. Structures in Seismic Regions - Design. Part 2 - Bridges. CEN 1994.

Casirati, M. & Franchioni, G. 1994. Seismic tests on a 1:8 model of an irregular bridge on three sha-king tables: model design and test planning. *Proc. 10th Europ. Conf. on Earthq. Engng.* Vienna..

Pinto, A. V., Verzeletti, G., Negro, P. & Guedes, J. 1995. Cyclic testing of a squat bridge pier. EUR Report (draft).

Muguruma, H. & Watanabe, F. 1990. Ductility improvement of high-strenght concrete columns with lateral confinement. *Proc., 2nd Int. Symp. on utilization of high strength concrete. Univ. of California.* Berkeley.

Sugano, S., Nagashima, T., Tamura, A. & Ichikawa, H. 1990. Experimental studies on seismic behaviour of reinforced concrete members of high strength concrete. *Proc., 2nd Int. Symp on utilization of high strength concrete. Univ. of California.* Berkeley.

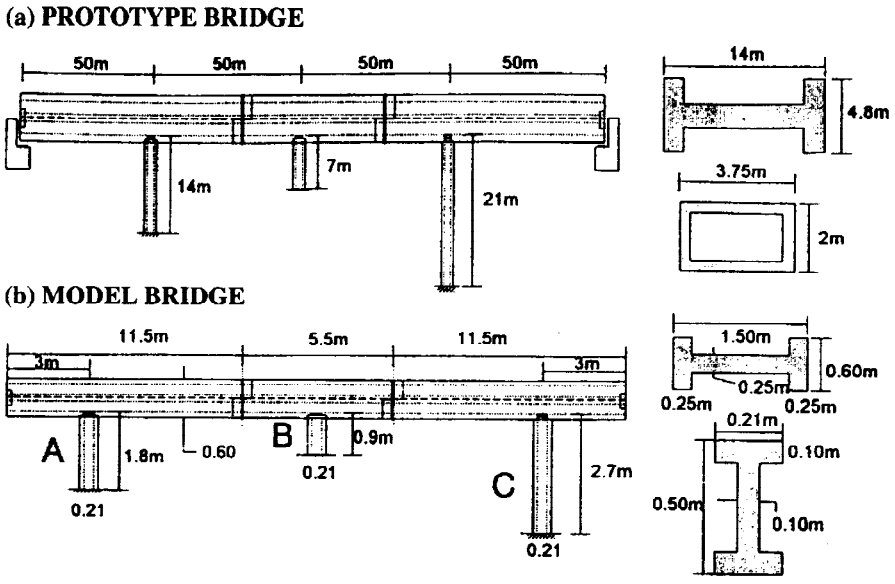

Fig. 1 - (a) Prototype bridge; (b) Model bridge specimen

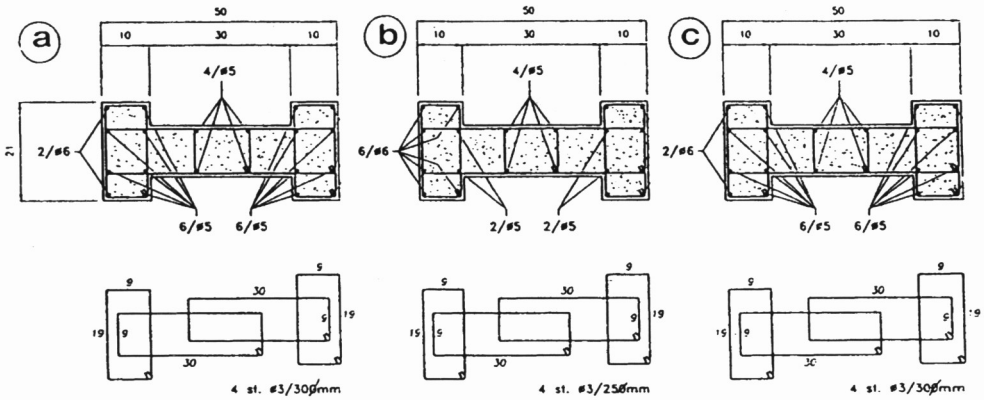

Fig. 2 - Reinforcing pattern; (a) pier A; (b) pier B; (c) pier C

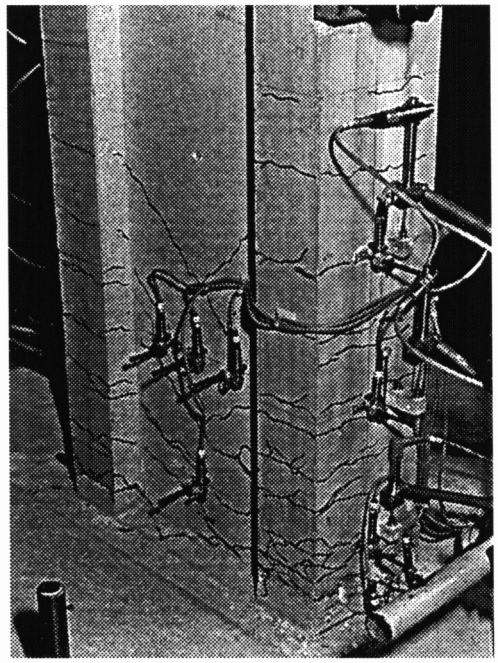

Fig. 3a - Pier after test

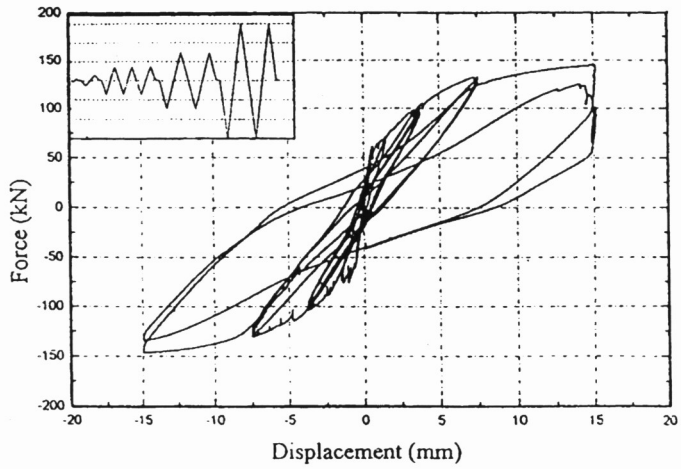

Fig. 3b - Loading path and hysteresis loops

Fig. 3 - Uniaxial flexure test of a squat pier

Table 2 - Bridge vibration frequencies and modes

Test	Frequency (Hz) Damping (%)															
Snap (Master)	2.6 (1.8)	3.5 (3.8)	4.5	5.1	—	9.7 (2.4)	12 (4.7)	—	17	20	23.5	—	35	37 (1.1)	—	—
Snap (Biax)	2.6	3.5 (3)	4.5	—	—	9.7 (1.4)	12 (4.5)	—	17	20		—	35	37 (0.4)	—	—
Snap (Ariete)	2.6	3.5 (2.6)	4.5	5.1	—	9.7 (1.5)	12 (2.7)	—	17	20	23.5	—	35	37 (0.9)	—	—
Sine (Master)	2.6 (1.3)	3.15	4.45	5.3	7.6	9.65 (2.9)	12.1 (3.7)	15 (1.1)	16.3 (3)	19.8 (0.7)	—	27.2 (1.3)	35.2 (0.7)	37.1	—	—
Sine (Biax)	2.6 (1.3)	3.10 (3)	4.2	5.2 (1.2)	7.5 (1.2)	9.55 (3)	12.3	15 (1.2)	16.5 (3)	19.8 (0.7)	—	27.1 (2.5)		—	—	—
Sine (Ariete)	—	3.22 (3.3)	4.5 (3.2)	—	7.5 (1.1)	9.64 (1.6)	12.1 (4.6)	14.8 (1)	16.6 (3)	19.8 (0.7)	—	27.1 (1.9)	35.2 (0.7)	37 (0.8)	—	—
Sine deck excit (vert)	—	—	4.5 (2.8)	5.1 (1.7)	7.4 (1)	9.8	12.3 (4.6)	—	16.2 (2.9)	19.8 (0.6)	22.5 (4.3)	27 (2)	35.2 (0.7)	36.7 (0.9)	53.2 (1.3)	65.1 (0.7)
Sine deck excit (Horiz)	—	3.17 (5)	—	5.2 (11)	7.4	9.8 (1.3)	12.2	—	16.9 (2.6)	19.7 (0.7)	—	27.2 (1.6)	35.3 (0.7)	36.4 (0.9)	53.4 (0.9)	65.5 (0.7)
Impact (cent)	2.6	—	—	5.1	7.4	9.7	12.1	15	—	19.8	23	27	—	37	53	65
Impact (eccen)	2.6	—	4.4	5.1	7.4	9.7	12.1	—	16	19.8	23	27	35.3	—	53	65
Mode	(L)	(Tr)	(Tr)	(V)	(V)	(Tr)	(R)	(V)	(Tr) (To)	(Tr)	(V)	(Tr) (To)	(Tr) (To)	(Tr)	(Tr) (To)	(Tr) (To)

(L): Longitudinal, (Tr): Transversal, (To): Torsional, (V): Vertical, (R): Rigid motion

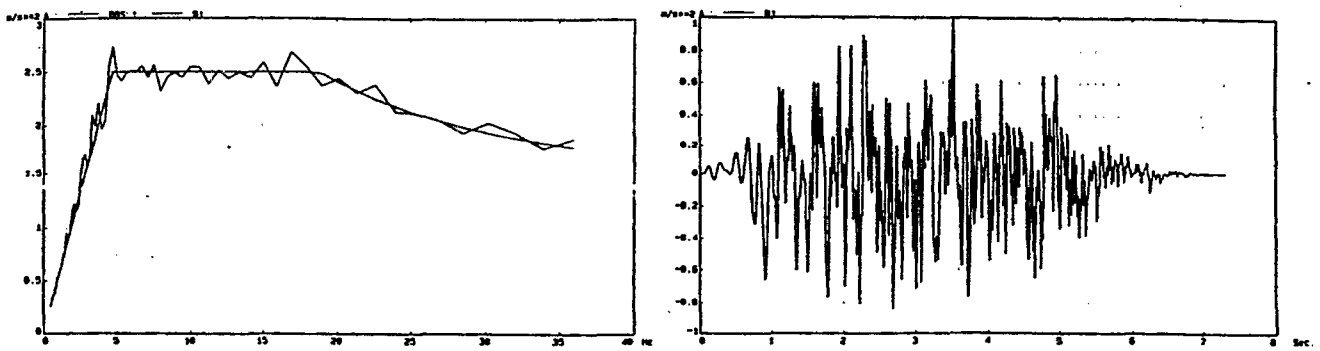

Fig. 5 - Input excitation (a) reference spectrum, (b) applied acceleration

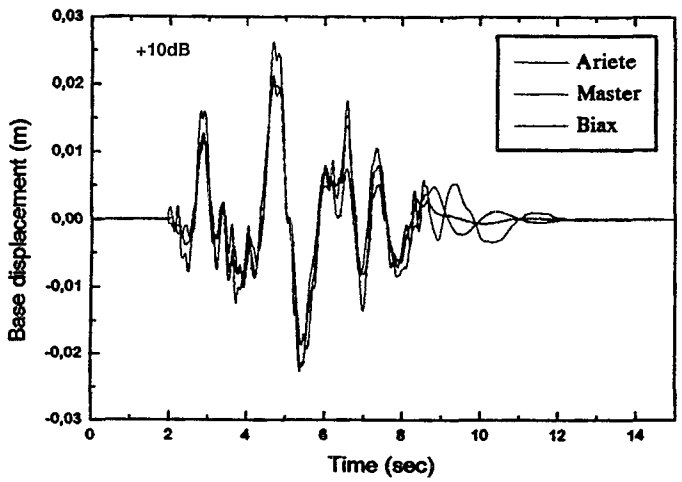

Fig. 6 - Base displacement

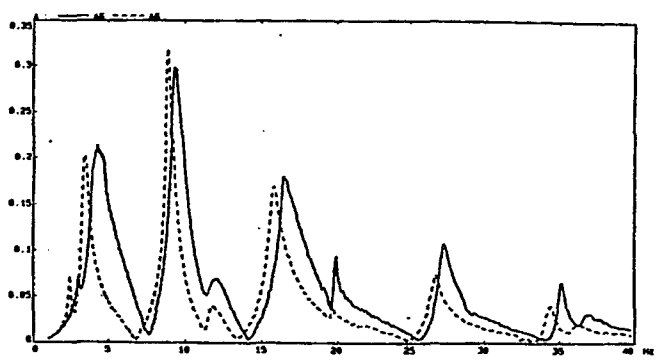

Fig. 7 - Frequency shift (pier on Master)